Volcanic eruptions, lightning, and a waterfall: Differentiating the menagerie of infrasound in the Ecuadorian jungle

Jeffrey B. Johnson,[1] Jonathan M. Lees,[2] and Hugo Yepes[3]

[1] In northeastern Ecuador, near Reventador Volcano, the airwaves are filled with infrasound. Here we identify the locations and characterize three distinct sources of local infrasound, including two types of infrasonic sources, which are not commonly discussed in the literature. The first of these novel sources is an intense and continuous radiator with a fixed location corresponding to San Rafael Waterfall. The signal from the river exhibits a tremor-like envelope that is well correlated across the 3-element infrasound network. Beyond the river, we also observe and map spatially variable sources corresponding to thunder. These transient signals have impulsive onsets, but are not well correlated across the network and are attributable to spatially-distributed source regions. Finally, we identify plentiful infrasound corresponding to Reventador's volcanic vent that is associated with unrest. This study demonstrates the utility of dispersed infrasound networks for distinguishing variable sources and improving interpretation of mechanisms of infrasound radiators. **Citation:** Johnson, J. B., J. M. Lees, and H. Yepes (2006), Volcanic eruptions, lightning, and a waterfall: Differentiating the menagerie of infrasound in the Ecuadorian jungle, *Geophys. Res. Lett.*, *33*, L06308, doi:10.1029/2005GL025515.

1. Introduction

[2] Low-frequency sound provides valuable constraints on earth processes as varied as volcanoes, ocean waves, earthquakes, and bolides [e.g., *Evers and Haak*, 2003; *Olson et al.*, 2003; *Johnson et al.*, 2004; *Le Pichon et al.*, 2004; *Willis et al.*, 2004]. Infrasonic sensing (i.e., sub-audible acoustics <20 Hz) is important because many geophysical sources are prolific radiators of high-energy, long-wavelength sound, which can propagate to regional and global distances with low intrinsic attenuation. Various types of natural earth and atmospheric sources efficiently perturb the atmosphere and induce low-frequency atmospheric airwaves. For instance, very large and/or long-duration sources (i.e., wind flowing over mountains or massive volcanic plume injections) can produce buoyancy waves with dominant very low frequencies <~0.01 Hz [e.g., *Ritsema*, 1980]. For somewhat smaller source regions and/or more instantaneous sources time functions, higher-frequency acoustic waves and shock waves are radiated. In the case of relatively low excess pressures ($\Delta P \ll 10^5$ Pa, corresponding to a low-intensity source or a site far from a stronger source), acoustic waves dominate because the atmosphere approximates an elastic medium [*Pierce*, 1981].

[3] Higher frequency acoustic waves tend to attenuate due to viscous dissipation, but at lower frequencies, particularly in the infrasonic bandwidth, they propagate efficiently and suffer signal diminution primarily through geometric spreading. For this reason, infrasound from very energetic sources is often easily detectable at regional or global distances (>100 km) [e.g., *Evers and Haak*, 2003; *Garces et al.*, 2005]. In this paper we focus on infrasound that is recorded locally, out to only about 10 km. At these offsets, higher frequency information is already weakened to the point where it is not audible to humans, but the infrasound is still exceedingly strong, in many cases exceeding 2 Pa at ~8 km (an equivalent SPL of ~100 dB).

[4] Infrasonic propagation, which affects both travel time arrivals and acoustic waveform, is affected by atmospheric temperature and wind structure [e.g., *Drob et al.*, 2003]. However, for sources generated locally, propagation paths can be considered nearly straight and these effects will be generally small. This implies that recorded acoustic waveforms may be used to robustly quantify geophysical source parameters, such as location and strength. As with seismic studies, our primary goal is to extract physical source parameters and for this we use techniques similar to those used in earthquake seismology. Fortunately, the analysis of infrasound is in some ways simpler because the atmosphere does not support shear waves, scattering is lessened at infrasonic wavelengths, and spatial variations in the atmospheric velocity structure are small relative to the wavelengths of interest [*Fleming et al.*, 1988].

2. Experiment

[5] We deployed a network of 3 infrasound-sensitive microphones at Reventador Volcano in July–August 2005 to better understand volcanological phenomena associated with the ongoing explosive eruptions. Serendipitously, during our volcano monitoring experiment, we discovered two additional types of infrasonic radiators that are unassociated with the volcanic activity. This paper provides an introduction to these non-volcanic sources as they have not typically been a focus in the existing acoustic or atmospheric sciences literature.

[6] Because our initial research goal was to study volcanic sources and acoustic attenuation, not locate events, our microphone network was deployed in a radial configuration east of the volcano with vent-sensor distances of 1.7 km (station RVEN), 3.5 km (station RLV3), and 7.6 km (station RHOT). The three sensors were identical electret condenser

---

[1]Department of Earth Sciences, University of New Hampshire, Durham, New Hampshire, USA.
[2]Earth Sciences Department, University of North Carolina, Durham, North Carolina, USA.
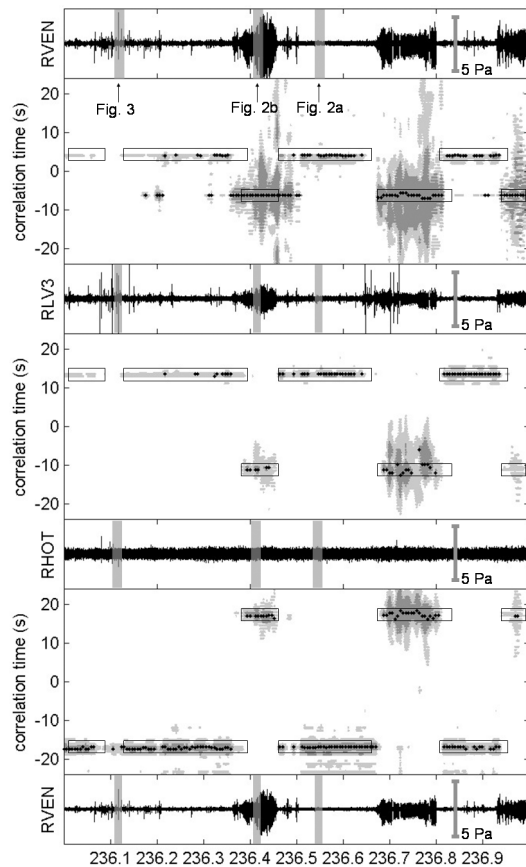[3]Instituto Geofisico, Escuela Politecnica Nacional, Quito, Ecuador.

Figure 1. Correlograms from August 24 (Julian day 236) comparing three different 24-hour acoustic traces. Grayscale intensity indicates relative cross-correlation values (>0.1, light gray and >0.2, dark gray). Small black circles represent peak cross-correlation values in excess of 0.2. Boxed areas denote periods of correlated (>0.1), consistent signals. Shaded segments indicate trace waveforms shown in detail in Figure 2 and Figure 3.

microphones (Larsen Davis model #2570 with preamp PRM900C), which possess a mostly flat response down to 0.27 Hz. We have analyzed continuous digital acoustic data (sampled at 125 Hz and later decimated to 25 Hz) during periods of time when all three stations were operational. Out of a two-month campaign, this includes more than 600 hours of acquisition when all stations were operating. We present data here from August 24 2005 (Julian day 236) during which we recorded examples of intense infrasonic transients and sporadic infrasonic tremor episodes superimposed upon a relatively weak, continuous tremor.

3. Analysis Methods

[7] For the analysis presented here, atmospheric structure is assumed to be reasonably homogeneous out to local distances (<10 km). As such, we presuppose that infrasound transients and tremor from point-source radiators will tend to be well correlated across our networks of sensors, which is found to be the case in our data from three separated microphones. Using the filtered trace data from the three stations, we search for maximum correlated signal in the time domain for a moving window. When the cross-correlation value for two compared waveforms surpasses an arbitrary threshold, we identify the corresponding time lag for that maximum cross-correlation trigger.

[8] The correlation threshold trigger can be set to different levels depending upon window comparison length, signal type, and signal-to-noise ratios. For the results presented here from August 24 the comparison windows were set at 1000 s (25000 samples) for data band-pass filtered between 2 and 12 Hz. In general, a minimum correlation value of 0.1 is appropriate for identifying weak, correlated infrasonic tremor on all three microphones. Low cross-correlation values are typical for relatively weak infrasound signal that is superimposed on strong short-duration signals or background noise [e.g., *Garces and Hetzer*, 2002]. However, such low correlation values are significant considering the long time duration (i.e., ~16 minutes) of the comparison windows. In general, we found correlation values to be much higher for intense transients and shorter-duration tremor, with correlation coefficients reaching as high as 0.9 (i.e., between RVEN and RLV3) and 0.3 (e.g., between RHOT and either of the two other stations).

[9] 'Correlograms' offer a graphical illustration of the temporal extent of correlated signal lags (Figure 1). Cross-correlation lags are calculated for all pairs of sensors (in our case, three) and when the sum of these lags approaches zero, we consider the signals to be consistent and appropriate for event location. This procedure is commonly applied to finite bandwidths during array processing of infrasound radiated from remote sources, utilizing four or more channels of data [e.g., *Evers and Haak*, 2003; *Garces et al.*, 2005].

[10] The ability to detect correlated signal from different sources is dependent upon the selected window length. For example, low-amplitude, long-duration sources benefit from an extended correlation window, whereas high-amplitude transients appear more clearly when short window lengths are utilized. Source detection can also be improved with selective filtering of waveforms. Removal of uncorrelated 'noise' through filtering will improve the likelihood that the correlation coefficients will be higher. Examples of correlated, filtered (2–12 Hz) infrasound signals from two different event types are shown in Figure 2. In many cases, waveform similarities are not easily identified visually (e.g., Figure 2a), but they stand out in the cross-correlation analyses.

[11] In the case of non-point sources, the correlation algorithm is not sufficient to identify signal because recorded waveforms are dissimilar and station-specific (Figure 3). In the case of thunder, for instance, energy is radiated from a dispersed source region corresponding to the spatial extent of the lightning, which is responsible for thermal shocking of the air [*Holmes et al.*, 1971]. This source dimension may be substantially larger than the wavelength of the infrasound, implying that a simple acoustic source approximation is inappropriate. In this case, we pick event arrivals manually by identifying the onset times of acoustic transients, that is, when energy clearly rises above background noise. This procedure is analogous to manual P-wave picks conducted in earthquake seismology.

[12] Both relative lag times and manual arrival time picks from the different stations are used to locate sources in
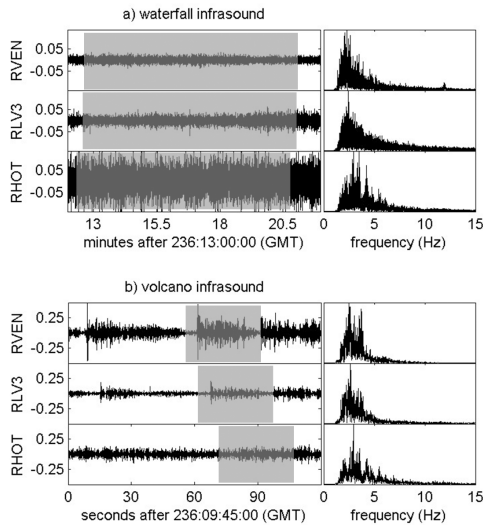
Figure 2. Acoustic pressure traces (in Pa), and corresponding amplitude spectra (normalized), for two distinct types of correlated signal (a) from San Rafael Waterfall and (b) from Reventador Volcano. Correlation lag delays, as determined in Figure 1, are indicated by shaded boxes.

space. This is fundamentally a different problem from traditional infrasound studies, where infrasound antennae are used to determine coherency of plane waves and hence back-azimuth to the acoustic source(s) [e.g., *Olson et al.*, 2003; *Garces et al.*, 2004]. In this study, we attempt to locate the various acoustic sources through a simple 3-D grid search (250 m resolution over a volume measuring 28 × 18 × 5 km) assuming a homogeneous sound velocity (340 m/s). Root mean square (RMS) timing errors are evaluated throughout the three dimensional grid for the different sources and those voxels with small RMS time residuals are then mapped (Figure 4). Although our network
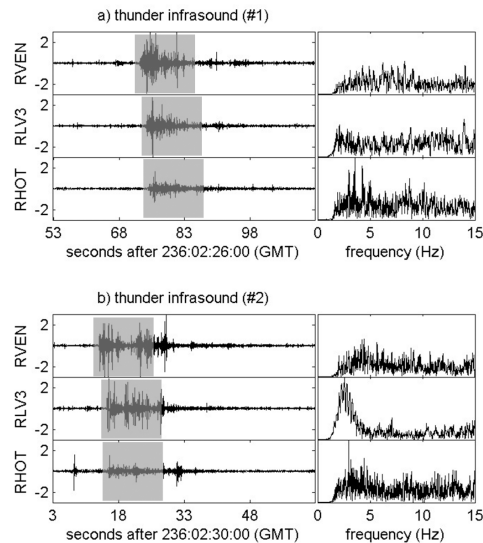
geometry is not an ideal configuration for precise source locations, especially outside of the network along the station axis, it is plainly suitable for distinguishing three main source regions. During August 24 we clearly identify a cone of potential sources aligned with the San Rafael Waterfall (e.g., Figure 2a), another cone of low RMS corresponding to the volcanic vent (e.g., Figure 2b), and a region of disparate source locations identified over a period of ~4 hours corresponding to a passing electrical storm (e.g., Figure 3).

4. Discussion

[13] As observed in previous studies [e.g., *Johnson et al.*, 2003], volcanic infrasound is found to be well-correlated across the local network, suggesting a component of point source infrasound radiation. In the case of Reventador, consistent acoustic lag times across the network indicate acoustic source(s) originating from one or more vents within the active cone (our network geometry is unable to distinguish between potential closely-spaced vents, such as those that exist at Stromboli Volcano [e.g., *Ripepe and Marchetti*, 2002]). In general, Reventador infrasound is suitably energetic such that many infrasonic transients are visually identifiable at the closer stations (Figure 2b). Although recorded excess pressures from Reventador Volcano can be as high as 100 Pa 1.7 km from the vent (Global Volcanism Program (2005), Reventador, *Bulletin of the Global Volcanism Network*, available at http://www.volcano.si.edu/world/volcano.cfm?vnum = 1502-01 = &volpage = var#bgvn_3008), typical infrasound recorded at station RHOT (7.6 km from the vent) is reduced in amplitude such that it is often obscured by other signals, especially from the waterfall, which is only 2 km distant. In these instances, cross-correlation techniques prove effective at identifying volcanic sources, such as extended-duration, low-amplitude volcanic tremor, which can be difficult to spectrally distinguish from wind-induced noise.

[14] Volcanoes are routinely studied with acoustic instrumentation, but river flow and electrical storms, with the
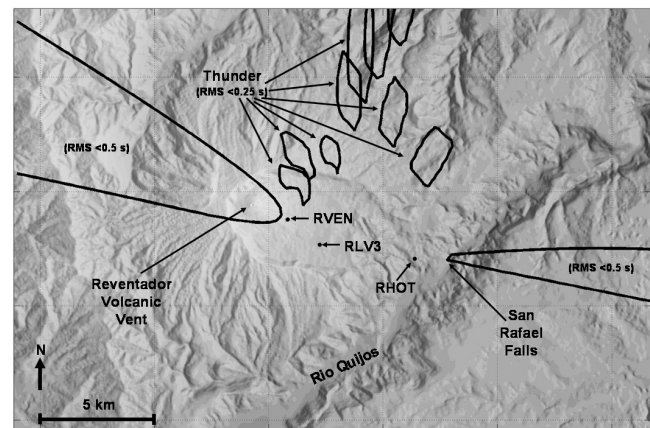

Figure 3. Acoustic pressure traces (in Pa), and corresponding amplitude spectra (normalized), for two different un-correlated thunder signals. Lag delays are indicated by shaded boxes with extent determined by manual arrival picks.

Figure 4. Shaded relief map of the Reventador region with contours denoting minimum RMS values for different sources. Waterfall and volcano regions correspond to RMS time residuals less than 0.5 s. Closed-loop thunder sources contours correspond to RMS time residuals less than 0.25 s.

exception of a few studies, have not been commonly investigated. Here we have identified a consistent radiator of infrasound from the vicinity of San Rafael Falls. This source is not surprising owing to the 145 m drop and considerable flow volume of the river, which should generate significant perturbations of the atmosphere. However, it is of interest that this infrasonic tremor is shown to be well-correlated across the infrasonic network out to about 8 km implying that at least a component of the source mechanism (i.e., the drum-like beating of water in the catch pool) can be characterized as a point source. Though this waterfall signal is continuous and well-correlated it is also relatively low in intensity (maximum $\Delta P \sim 0.05$ Pa at RVEN; 7.8 km) compared to the August 24 volcanic infrasound ($\Delta P \sim 1$ Pa at RVEN; 1.7 km from vent). Thus the waterfall infrasound is obscured when the volcano is radiating intensely.

[15] The thunder source is unique in that it is very broadband (e.g., extending above 20 Hz) and not correlated across the network. For example, the high-amplitude acoustic waveforms shown in Figure 3 ($\Delta P > 2$ Pa at all stations) are dissimilar at the different stations, implying a temporally and/or spatially-dispersed source. Because the onset of these discrete transients are impulsive and easily 'picked', the variations in their relative arrival times may be used to map the dynamic locations of successive lightning. Further information about the precise spatial extent of the lightning would be improved with a more dispersed network of microphones.

5. Conclusion

[16] We identify and comment on the spatial variability and strength of acoustic signals associated with volcanoes, river flow, and electrical storms using a rudimentary 3-element infrasonic network. For the electrical storm sources the broad aperture of our network permits reasonably precise source localizations, including both azimuth and distance constraints, because the events occurred off the axis of the 3-element network. In contrast, both the volcano and waterfall source are more vaguely located within a back-azimuth cone. Clearly, this type of study could benefit from sensor geometries with more microphones and greater spatial distribution around the periphery of the study region. Future deployments with improved network geometry will be valuable for identifying and precisely locating these and other types of locally-produced infrasound.

References

Drob, D. P., J. M. Picone, and M. Garces (2003), Global morphology of infrasound propagation, *J. Geophys. Res.*, *108*(D21), 4680, doi:10.1029/2002JD003307.

Evers, L. G., and H. W. Haak (2003), Tracing a meteoric trajectory with infrasound, *Geophys. Res. Lett.*, *30*(24), 2246, doi:10.1029/2003GL017947.

Fleming, E. L., S. Chandra, M. R. Shoeberl, and J. J. Barnett (1988), Monthly mean global climatology of temperature, wind, geopotential height and pressure for 0–120 km, *NASA Tech. Memo. 100697*, 91 pp.

Garces, M. A., and C. Hetzer (2002), Evaluation of infrasonic detection algorithms, paper presented at 24th Seismic Research Review, Off. of Nonproliferation Res. and Dev., Orlando, Fla.

Garces, M., H. Bass, D. Drob, C. Hetzer, M. Hedlin, A. Le Pichon, K. Lindquist, R. North, and J. Olson (2004), Forensic studies of infrasound from massive hypersonic sources, *Eos Trans. AGU*, *85*(43), 440–441, 433.

Garces, M., P. Caron, C. Hetzer, A. Le Pichon, H. Bass, D. Drob, and J. Bhattacharyya (2005), Deep infrasound radiated by the Sumatra earthquake and tsunami, *Eos Trans. AGU*, *86*(35), 317.

Holmes, C. R., M. Brook, P. Krehbiel, and R. A. McCrory (1971), On the power spectrum and mechanisms of thunder, *J. Geophys. Res.*, *76*, 2106–2115.

Johnson, J. B., R. C. Aster, M. C. Ruiz, S. D. Malone, P. J. McChesney, J. M. Lees, and P. R. Kyle (2003), Interpretation and utility of infrasonic records from erupting volcanoes, *J. Volcanol. Geotherm. Res.*, *121*(1–2), 15–63.

Johnson, J. B., R. C. Aster, and P. R. Kyle (2004), Volcanic eruptions observed with infrasound, *Geophys. Res. Lett.*, *31*, L14604, doi:10.1029/2004GL020020.

Le Pichon, A., V. Maurer, D. Raymond, and O. Hyvernaud (2004), Infrasound from ocean waves observed in Tahiti, *Geophys. Res. Lett.*, *31*, L19103, doi:10.1029/2004GL020676.

Olson, J. V., C. R. Wilson, and R. A. Hansen (2003), Infrasound associated with the 3 November, 2002 Denali Fault, Alaska earthquake, *Geophys. Res. Lett.*, *30*(23), 2195, doi:10.1029/2003GL018568.

Pierce, A. D. (1981), *Acoustics: An Introduction to Its Physical Principles and Applications*, 642 pp., McGraw-Hill, New York.

Ripepe, M., and E. Marchetti (2002), Array tracking of infrasonic sources at Stromboli volcano, *Geophys. Res. Lett.*, *29*(22), 2076, doi:10.1029/2002GL015452.

Ritsema, R. (1980), Observations of Mount St. Helens eruption, *Eos Trans. AGU*, *61*, 1201–1202.

Willis, M., M. A. Garces, C. Hetzer, and S. Businger (2004), Infrasonic observations of open ocean swells in the Pacific: Deciphering the song of the sea, *Geophys. Res. Lett.*, *31*, L19303, doi:10.1029/2004GL020684.

————————
J. B. Johnson, Department of Earth Sciences, University of New Hampshire, Durham, NH 03824, USA. (jeff.johnson@unh.edu)

J. M. Lees, Earth Sciences Department, University of North Carolina, Durham, NC 27599-3315, USA.

H. Yepes, Instituto Geofisico, Escuela Politecnica Nacional, Quito, Ecuador.